Removal Kinetic of Cationic Dye Using Poly (Sodium Acrylate)-Carrageenan/Na-Montmorillonite Nanocomposite Superabsorbents

Gholam Reza Mahdavinia[1]*, Roghaye Zhalebaghy[2]

[1]*Department of Chemistry, Faculty of Science, University of Maragheh, P.O. Box 55181-83111, Maragheh, Iran*
[2]*Department of Chemistry, Faculty of Science, Islamic Azad University, Ahar Branch, Ahar, Iran*

Abstract

Nanocomposite superabsorbents were prepared from solution polymerization of sodium acrylate in the presence of carrageenan biopolymer and sodium montmorillonite nanoclay. The optimum swelling of nanocomposite superabsorbents was achieved at 8 wt% of sodium montmorillonite nanoclay. Clay-free superabsorbent and nanocomposite containing 8 wt% of nanoclay were evaluated to remove cationic crystal violet dye from water. It was found that by inclusion of nanoclay into carrageenan-based superabsorbent not only the rate of dye adsorption is increased, but also the removal efficiency is enhanced by 11 %. The results indicated that the experimental data fit the Freundlich isotherm the best.
Keywords: Nanocomposite, Superabsorbent, Dye Removal, Kinetic, Carrageenan

1. Introduction

Industry is a huge source of water pollution; it produces pollutants that are extremely harmful to people and the environment. Colored water and solutions containing toxic heavy metals from many industries like dye, textile, paper, plastic, plating, and mining facilities produce considerable polluted waters. The pollutions must be removed from wastewater before discharging it into the environment. Adsorption process, an inexpensive and simple design, can be used to remove of dye contaminations from aqueous environments [1]. Superabsorbents are type of three-dimensional hydrophilic polymers capable to swell and absorb a large amount of water [2]. They are found to be valuable in some specialized applications, including controlled delivery of bioactive agents [3] and wastewater treatment [4]. Superabsorbents can classify into non-ionic and ionic materials. The ionic types comprise anionic ($-CO_2^-$, $-SO_3^-$) or cationic ($-NR_3^+$) pendants [5]. The presence of these ionic groups in the superabsorbents opens potential area of application that is related to remove of pollutants from wastewaters [6]. The adsorption of dyes onto adsorbents takes place through the electrostatic attractions between opposite charges of adsorbents and pollutants. But, these superabsorbents mainly do not possess enough strength. Introducing of nano-clays into hydrogel compositions can be considered as one of the methods to improve this property of superabsorbents [7]. It has been reported that inclusion of nano-clays in the superabsorbent composition not only their strength can improve but also the rate and dye adsorption capacity will be increased [8]. Nanocomposites superabsorbents containing Na-montmorillonite [9], laponite [10], attapulgite [11], and sepiolite [12] have been synthesized and used to remove pollutions from aqueous media. Also, due to non-toxicity and biodegradability of biopolymers, the removal of dyes from water has been evaluated by using nanocomposite superabsorbents based on polysaccharides biomasses [13].

Because of eco-friendly property of carrageenan with $-SO_3^-$ groups, we attempted to synthesize of nanocomposite superabsorbents by introducing of this biopolymer. The present work describes the synthesis of

crosslinked poly (sodium acrylate) in the presence of carrageenan biopolymer and sodium montmorillonite nanoclay. The structure of nanocomposite superabsorbents was investigated using FTIR, XRD, and SEM technique. The effect of nanoclay on the water absorbency of nanocomposites was studied. The capability of the so-obtained nanocomposite superabsorbents was examined to remove cationic crystal violet dye (Scheme 1) from water.
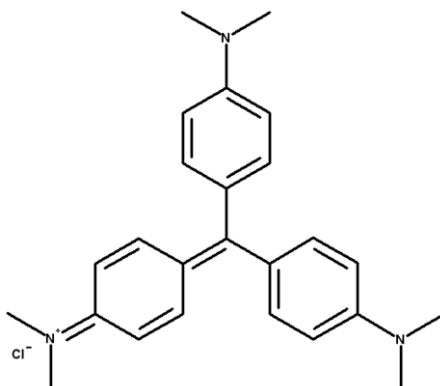
Scheme 1 Structure of cationic crystal violet dye

2. Experimental

2.1. Materials

kappa-Carrageenan was obtained from Condinson Co., Denmark. N,N-methylenebisacrylamide (MBA) and ammonium persulfate (APS) from Fluka, were of analytical grade and were used as received. Acrylic acid (Merck) was used without further purification. Natural sodium-montmorillonite (sodium Cloisite, Na-MMt) as a clay with cation exchange capacity of 92 meq/100 g of clay was provided by Southern Clay Products. All other ingredients were analytical grades and were used as received.

2.2. Synthesis of nanocomposite superabsorbents

The nanocomposite superabsorbents were synthesized by varying the clay content from 0 to 15 wt% while the other reaction variables kept constant. The suffix *m* in Clay*m* will show the wt% of Clay in nanocomposites composition. In general, clay (0, 0.25, 0.5, 0.75, and 1 g) was dispersed in 30 mL of distilled water and sired under magnetic stirrer for 24 h. Dispersed clay solution was transferred in a one-liter reactor equipped with mechanical stirrer. To control the reaction temperature, the reactor was placed in a water bath preset at 60 $^{\circ}$C. Then, 0.5 g of carrageenan was added to the solution containing clay and stirred for 2 h until completion of dissolution. AA was neutralized up to 80 % neutralization degree using NaOH 10 wt% at 0 $^{\circ}$C, and MBA (0.1 g) was dissolved in neutralized acrylic acid (e.g. sodium acrylate, Na-AA) and were simultaneously added into polymerization solution and allowed to stir for 1 h. Finally, APS (0.1 g in 2 mL of water) as initiator was added into solution and stirred until superabsorbents formation. After this time, the nanocomposites were dried at ambient temperature for 1 week the dried samples were milled and sieved to 40-60 mesh sizes and kept away from light and moisture.

2.3. Swelling Measurements

The degree of swelling (DS) was determined by immersing the dried nanocomposite superabsorbents (0.1 g) in distillated water (100 mL) and was allowed to soak for 24 h at room temperature. After this time, they were removed from the water, blotted with filter paper to remove surface water, weighed and the DS (g water/g dried nanocomposite) was calculated using Eq (1):

$$DS = \frac{W_s - W_d}{W_d} \quad (1)$$

where W_s and W_d are the weights of the samples swollen in water and in dry state, respectively.

2.4. Gel Content
0.2 g of nanocomposites was immersed in distilled water for 72 h, then swollen nanocomposites were filtered, dewatered with 200 ml ethanol and dried at 70 °C for 5 h. Dried samples weighed and gel content (*Gel %*) was calculated by Eq 2.

$$Gel\% = \frac{m}{M} \times 100 \quad (2)$$

where m and M stand for final and initial weight of the sample, respectively.

2.5. Dye Adsorption Measurements
Dye adsorption was carried out by immersing the 0.05 g of nanocomposites into 50 mL of dye solution with 30 mg/L of CV solution. All adsorption experiments were examined through a batch method on a stirrer with a constant speed at 120 rpm. To study the adsorption kinetics, at specified time intervals, the amount of adsorbed CV was evaluated using a UV spectrometer at λ_{max}=590 nm. The content of adsorbed dye (q_t, mg/g) was calculated using following Eq 3:

$$q_t = \frac{(C_0 - C_t)}{m} \times V \quad (3)$$

where, C_0 is the initial CV concentration (mg/L), C_t is the remaining dye concentrations in the solution at time *t*, *V* is the volume of dye solution used (L), and *m* is the weight of nanocomposite (g). Adsorption isotherm was carried out by immersing of 0.05 g of nanocomposites into 50 mL of dye solutions with 10, 20, 30, 40, and 50 mg/L of CV for 24 h. The equilibrium adsorption capacity of nanocomposites, q_e (mg/g), was determined using Eq 3. At this Eq, the C_t and the q_t will be replaced with equilibrium concentration of dye in the solution (C_e) and equilibrium adsorption capacity (q_e), respectively.

2.6. Instruments
Dried nanocomposite was coated with a thin layer of gold and imaged in a SEM instrument (Vega, Tescan). One-dimensional, wide angle X-ray diffraction patterns were obtained by using a Siemens D-500 X-ray diffractometer with wavelength, λ=1.54Å (Cu-Kα), at a tube voltage of 35 KV, and tube current of 30 mA. The FTIR spectra were performed using ABB Bomem spectrophotometer (KBr pellets).

3. Results and Discussions
3.1. Synthesis and Characterization
Solution polymerization of partially neutralized acrylic acid was carried out in the presence of carrageenan biopolymer and sodium montmorillonite nanoclay. APS and MBA were used as initiator and crosslinker, respectively. The persulfate initiator is decomposed under heating to generate sulfate anion-radical. Then, the sulfate anion-radical abstracts hydrogen from H_2O molecules to produce hydroxyl radicals [14]. The polymerization of sodium acrylate can initiate in the presence of hydroxyl radicals. In the presence of a cross-linker, i.e. MBA, cross-linking reaction can occur and finally a three dimensional network is produced. Carrageenan biopolymer and dispersed Na-MMt sheets will capture into crosslinked poly (sodium acrylate) (Scheme 2).
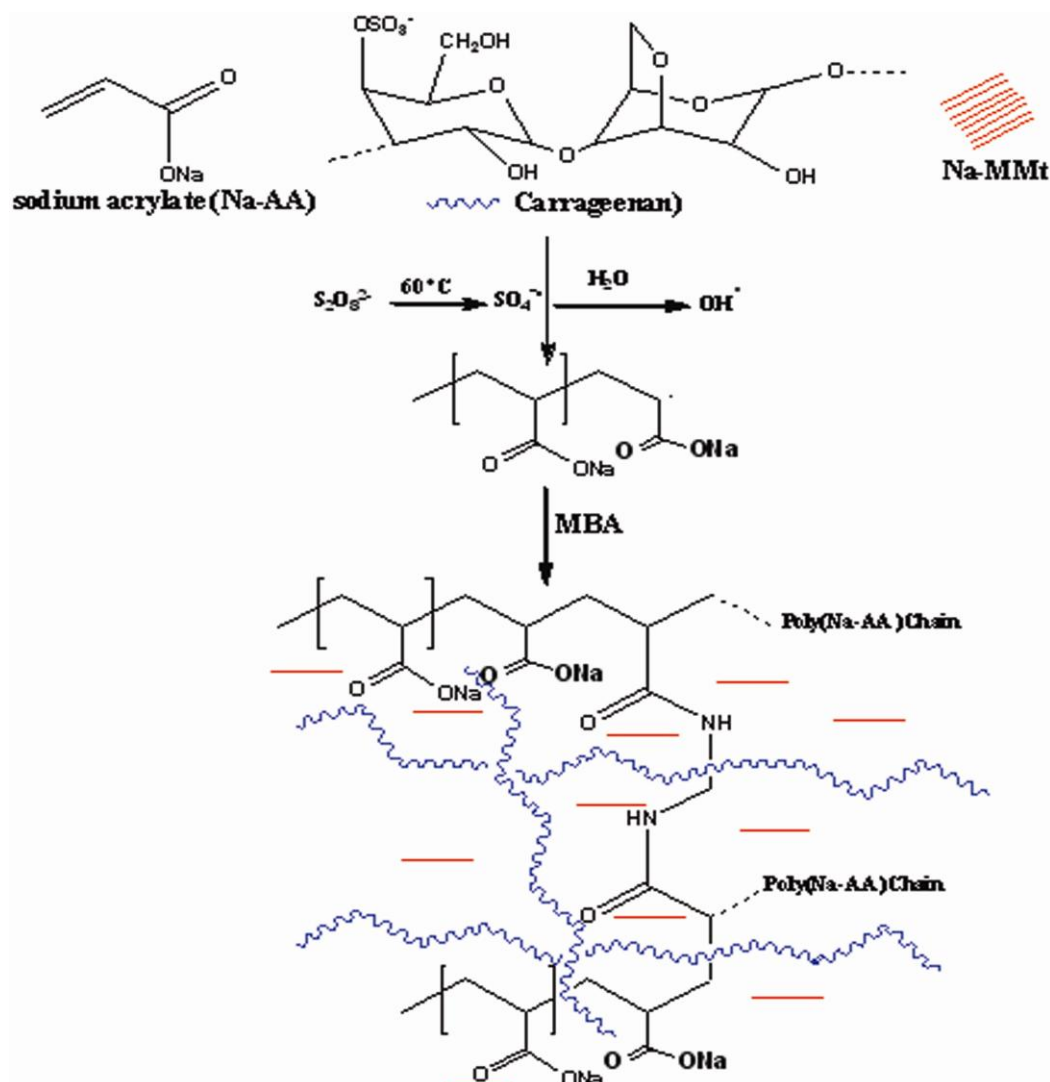
Scheme 1 A simple mechanism of synthesis of nanocomposite superabsorbent

The type of dispersion of nanoclay in the superabsorbents matrix was studied using XRD technique. We attempted to investigate the XRD patterns of nanocomposites by varying the clay content and the results are shown in Figure 1. The XRD profile of pristine Na-MMt (Figure 1a) shows a strong diffraction peak at $2\theta =$ 7.6 corresponding to the distance of clay sheets with d spacing 11.61 A˚. The XRD patterns of nanocomposites are shown in Figure 1b-d. No distinct diffraction peak was appeared in the XRD patterns of nanocomposites and it can be concluded that the clay layers are completely exfoliated. Similar observations for nanocomposite superabsorbents containing Na-MMt nanoclay and Na-AA monomer have been reported and the XRD studies of related nanocomposites have showed exfoliated structures [15, 16].

The structure of Nanocomposites was studied using FTIR spectra. The spectra of pristine clay, carrageenan, and nanocomposite are illustrated in Figure 2. In the pristine clay spectrum (Figure 2a), the characteristic peaks at 3634, 3448, 1638 and 1041 cm^{-1} are assigned to (-OH stretch from lattice hydroxyl, -OH stretch from free H$_2$O, -OH bending and Si-O stretch, respectively. The FTIR of carrageenan (Figure 2b) shows characteristic bands at 3000-3418 and 1373 cm^{-1} due to the of O-H and sulfate stretch, respectively. The peaks at 1026, 918, and, 841 cm^{-1} are attributed to the glycoside linkage, 3,6- anhydro-D-galactose, and C-O-S in galactose segments, respectively. The FTIR of nanocomposite Clay8 containing MMt, carrageenan, and poly (sodium acrylate) components was shown in Figure 2c.
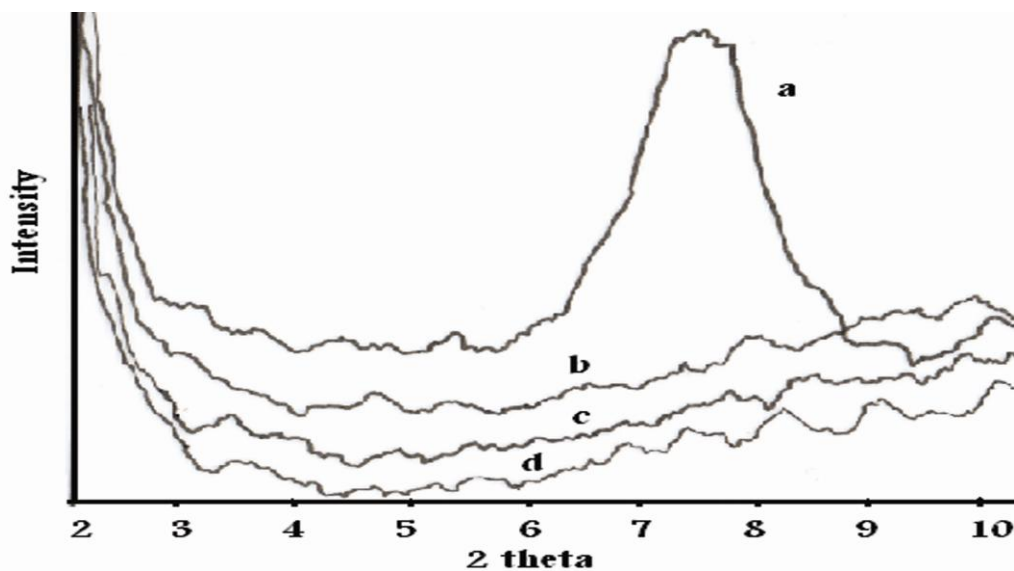
Figure 1 XRD profiles of (a) pristine clay and nanocomposites containing (b) 4.2, (c) 8, and (d) 15 wt% of Na-MMt nanoclay.

As can be seen from the figure, the characteristic peak at 3634 cm^{-1} correspondence to MMt disappeared and this observation shows the interaction of clay and polymer functional groups. The peak at 1041 cm^{-1} due to Si-O stretch confirms the presence of clay in the nanocomposite composition. The presence of carrageenan component in the nanocomposite is confirmed by a peak at 1311 cm^{-1} due to sulfate stretch. On comparing to pure carrageenan, this peak shows a shifting and may be attributed to the interaction of sulfate groups by other functional groups of nanocomposite. Poly (sodium acrylate) chains carry carboxylate functional groups. The carboxylate groups are confirmed by the band characteristics at 1574 cm^{-1} due to asymmetric stretching in carboxylate anion that is reconfirmed by another peak at 1412 cm^{-1} which is related to the symmetric stretching mode of the carboxylate anion.
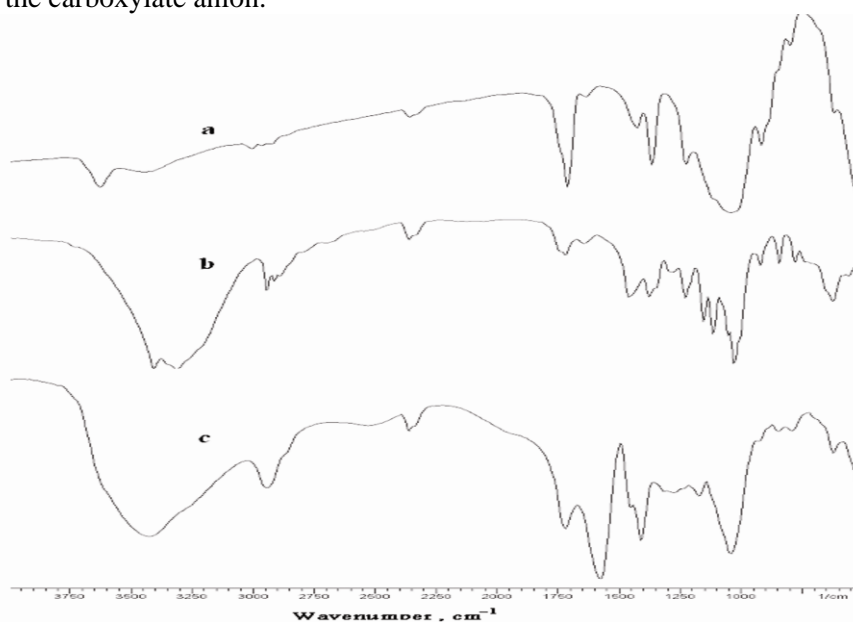
Figure 2 FTIR spectra of (a) pristine clay, (b) carrageenan biopolymer, and (c) Clay8 nanocomposite superabsorbent.

Figure 3 shows the SEM micrographs of clay-free hydrogel and Clay8 nanocomposite. While the hydrogels without clay shows a relatively tight surface (Figure 3a), the nanocomposite (Figure 3b) contain coarse and undulant surface.
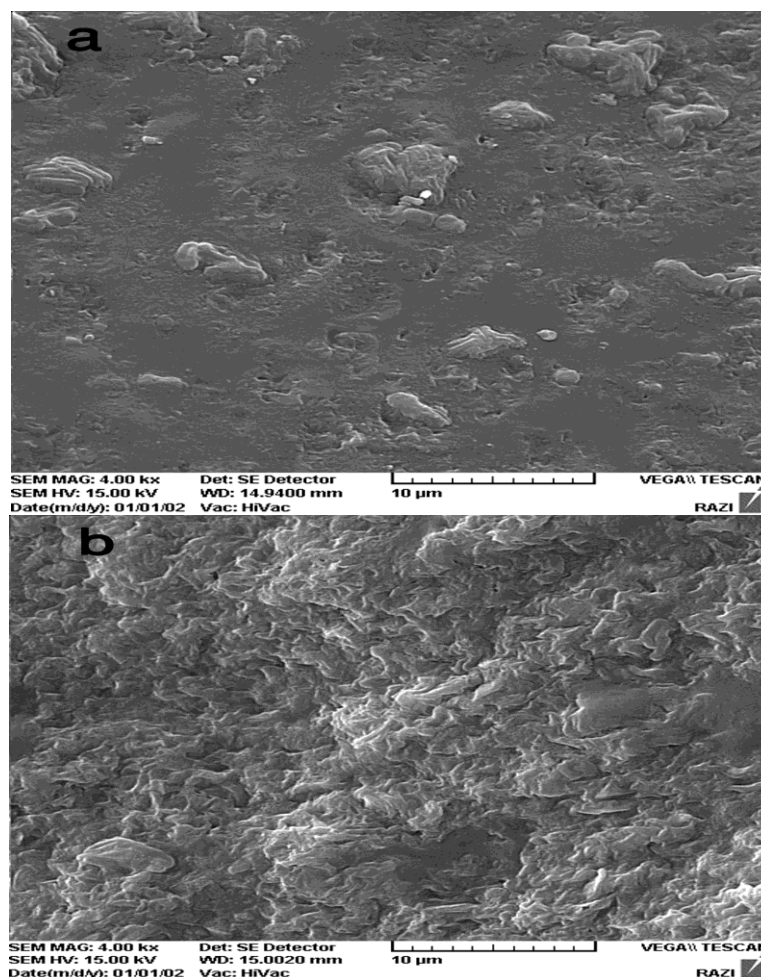
Figure 3 SEM micrographs of (a) clay-free superabsorbent and (b) Clay8 nanocomposite superabsorbent

3.2. Swelling of Nanocomposites

Degree of swelling of nanocomposites was investigated by changing the clay content while the other reaction variables kept constant. As it is evident form Figure 4, by changing the clay content up to 8 wt%, the water absorbency of nanocomposites increased. Maximum water absorbency (173 g/g) was obtained for nanocomposite with 8 wt% of Na-MMt nanoclay (Clay8). I fact, increasing the Na-MMt content up to 8 wt% improved water absorbency of nanocomposite.

The corresponding increase in swelling up to 8 wt% of MMt could be attributed to increase in ionic osmotic pressure of nanocomposites. This osmotic pressure is due to the mobile ions on the nanoclay particles [17]. When the amount of Na-MMt in the nanocomposite composition was increased from 8 to 15 wt% of nanoclay, a decrease in water absorbency was found. The gel contents of nanocomposite containing different amounts of Na-MMt were determined and the results are shown in Figure 4. While the change in gel content was not notable up to 8 wt% of nanoclay, it was significantly decreased when the clay content increased above 8 wt%. The gel contents of Clay11.6 and Clay15 samples showed a decrease of 7.5 and 13.5 wt% compared with Clay8. By decreasing the gel content, swelling capacity will decrease. In fact, by further increase in Na-MMt content, the viscosity of polymerization medium will increase and restrict the macroradicals movement;

thereby decreasing the gel content and subsequently, the water absorbency content will decrease. The other reason to reduce in water absorbency by increasing of clay content can be attributed to act of nanoclay as multifunctional crosslinker [18]. More crosslinking points causes to the higher crosslinking density and decreases the space between the copolymer chains and consequently, the resulted highly crosslinked rigid structure cannot be expanded and hold a large quantity of water. A similar behavior have been reported by Al et al in the case of starch-g-acrylic acid/An-MMt nanocomposite hydrogels [19].
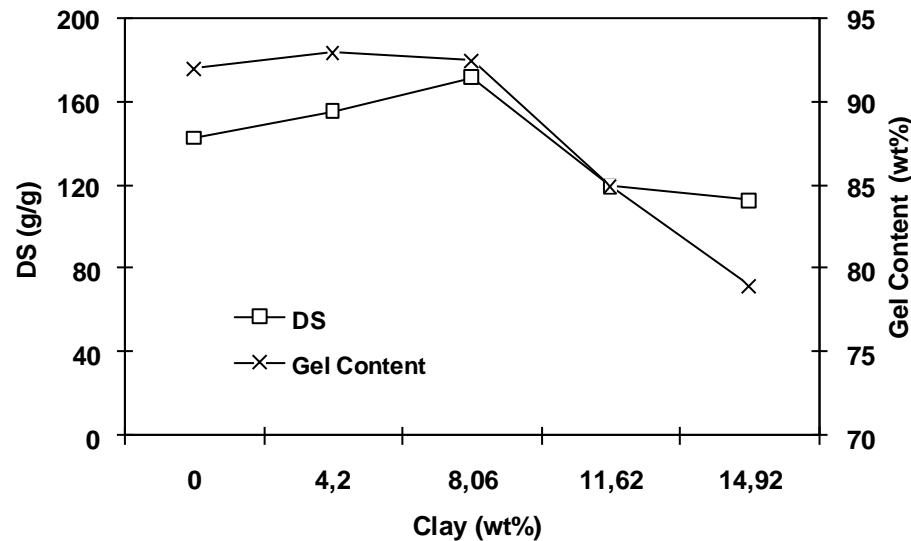
Figure 4 Influence of Na-MMt nanoclay on the water absorbency capacity and gel content of carrageenan-based nanocomposite superabsorbents

In practical applications, not only a higher swelling capacity is required, but also a higher swelling rate is needed. Buchholz has suggested that the swelling kinetics for the superabsorbent is significantly influenced by factors such as swelling capacity, size distribution of powder particles, specific size area and composition of polymer [20]. Figure 5 represents the dynamic swelling behavior of synthesized nanocomposites with different clay content in water. Initially, the rate of water uptake sharply increases and then begins to level off. According to results, the swelling kinetic of the nanocomposites is significantly influenced by the clay amount. A power law behavior is obvious from Figure 5. The data may be well fitted with a Voigt-based equation (Eq.4) [21]:

$$S_t = S_e(1 - e^{-t/\tau}) \quad (4)$$

where S_t (g/g) is swelling at time t, S_e is equilibrium swelling (power parameter, g/g); t is time (min) for swelling S_t, and τ (min) stands for the "rate parameter". The smaller τ values indicate the faster swelling process.

The rate parameters for prepared nanocomposites with different clay content are illustrated in Table 1. By inclusion of Na-MMt nanoclay into hydrogels up to 8 wt%, an increase in rate of water uptake is observed. The increase in the rate of absorption would be expected from the increase in osmotic pressure of nanocomposites due to mobile ions in Na-MMt. Above 8 wt% of Na-MMt, the rate parameter was decreased. The decrease in rate parameter may be attributed to the interaction between polymer chains and clay that prevent ease of expansion of polymer chains. In fact, the presence of Na-MMt nanoclay in the nanocomposites up to 8 wt% can relatively improve the rate parameter.
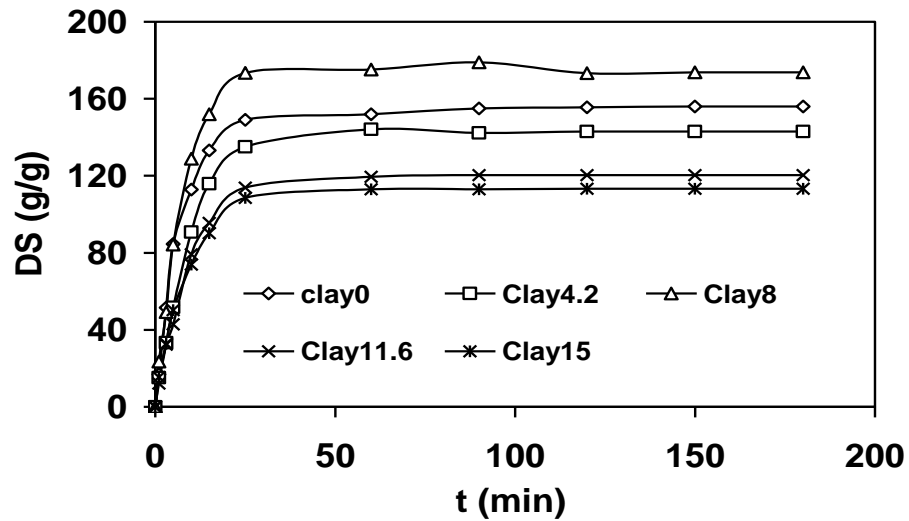
Figure 5 Dynamic swelling kinetic of nanocomposite superabsorbents containing different clay content

Table 1 τ values (s) for nanocomposite superabsorbents

	Clay0	Clay4.2	Clay8	Clay11.6	Clay15
τ, s	492	486	420	525	501

3.3. Dye Adsorption Study

The structural property of adsorbents is important parameter that can affect the adsorption speed of adsorbate onto adsorbents [22]. So, we tried to investigate the effect of Na-MMt nanoclay on the dye adsorption speed. Clay-free hydrogel (Clay0) and nanocomposite hydrogel containing 8 wt% of Na-MMt nanoclay (Clay8) were examined to dye adsorption study. The effect of time on the dye adsorption capacity of carrageenan based superabsorbents is depicted in Figure 6.
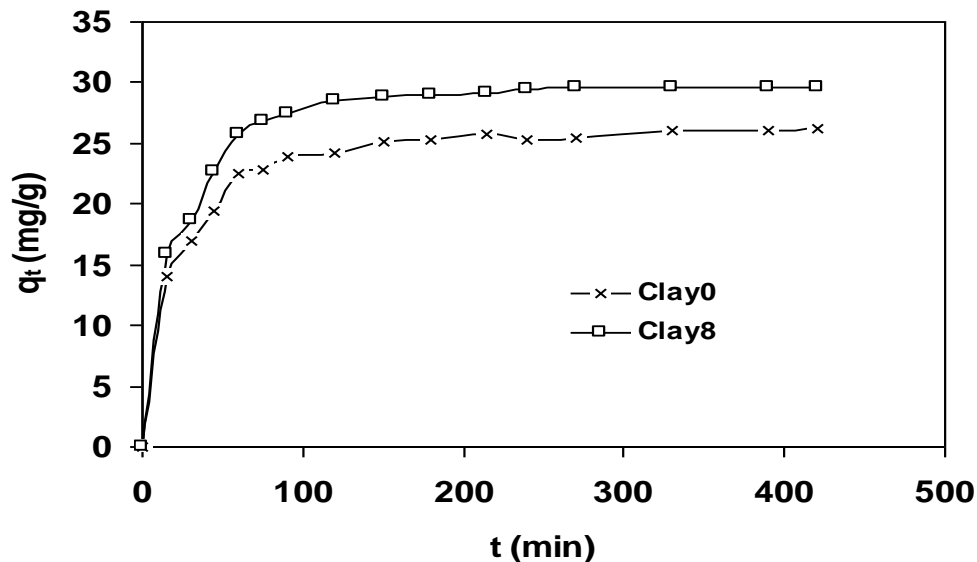
Figure 6 Dye adsorption speeds of clay-free hydrogel and clay8 nanocomposite (0.05 g of samples in 50 mL of dye solution with 30 mg/L of CV)

As it is clear from figure, the dye adsorption speed is affected by hydrogel composition. Inclusion of Na-MMt into hydrogel caused an increment in dye adsorption speed. During 120 min, the removal efficiency of Clay0 and Clay8 is 80 and 95 %, respectively. In fact, according to results, dye adsorption speed improved by introducing the Na-MMt nanoclay in hydrogel composition. In a further studying on the dye adsorption by hydrogels, the experimental data fitted by both pseudo-first-order and pseudo-second-order kinetic models. The pseudo-first-order kinetic model is expressed as below [23]:

$$Ln(q_e - q_t) = Lnq_e - k_1 t \quad (5)$$

where, q_e and q_t (mg/g) are the amount of adsorbed dye on the nanocomposites at equilibrium and at time t, respectively. k_1 (min^{-1}) presents the rate constant of first-order adsorption.
The pseudo-second-order kinetic model is given as below [23]:

$$\frac{t}{q_t} = \frac{1}{k_2 q_e^2} + \frac{t}{q_e} \quad (6)$$

where, k_2 (g/mg.min) is rate constant of second-order adsorption and q_e is the theoretical adsorbed dye (mg/g) that can be calculated from pseudo-second-order.
In order to obtain model calculations, we can plot $Ln(q_e-q_t)$ against t for pseudo-first-order and $\frac{t}{q_t}$ against t for pseudo-second-order. Model calculations for all nanocomposites were given in Table 2. It was found that the plotting of $\frac{t}{q_t}$ against t gives a straight-line with a high correlation coefficient (R^2>0.999) and it can be concluded that adsorption kinetic of dye by clay-free superabsorbent and nanocomposite superabsorbent has the best fitting to the pseudo-second-order (Figure 7).
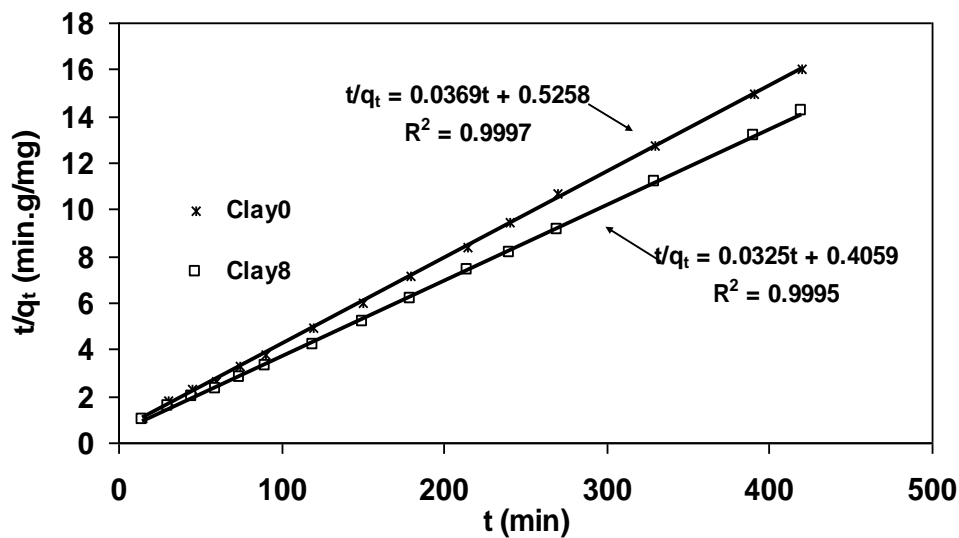
Figure 7 Adsorption kinetic of the CV onto the clay-free superabsorbent and Clay8 nanocomposite according to pseudo-second-order model

Table 2 The pseudo first-order and pseudo second-order rate parameters for CV adsorption by clay-free superabsorbent and nanocomposite superabsorbent.

	First-order kinetics				Second-order kinetics			
	q_e, Theor., mg/g	q_e, Exp., mg/g	$k_1 \times 10^3$, min^{-1}	R^2	q_e, Theor., mg/g	q_e, Exp., mg/g	$k_2 \times 10^3$, g/mg.min	R^2
Clay0	11.9	26.2	15.2	0.964	27.1	26.2	2.58	0.9997
Clay8	13.65	29.6	82	0.951	30.7	29.6	2.61	0.9995

As can be seen from the data, according to pseudo-second-order kinetic, the experimental and theoretical equilibrium adsorption capacities of hydrogel and nanocomposite hydrogel are in agreement. Although the dye adsorption kinetic dos not follow the first-order kinetic at the best, but the k_1 values indicate that the presence of nanoclay caused a significant increment in dye adsorption rate. This information confirms the results of Figure 6.

3.4. Adsorption isotherms
The adsorption of CV onto hydrogel and nanocomposite hydrogel as a function of initial dye concentration was studied by immersing 0.05 g into dye solution with concentrations ranging from 10-50 mg/L. The adsorption isotherms describe the optimize adsorption system as well as the effectiveness of adsorbents [16]. In fact, it is important to investigate to obtain an optimum isotherm model indicating the CV adsorption system onto nanocomposite hydrogels. The practical data were fitted to the Langmuir and Freundlich models. In the Langmuir adsorption model, adsorption of adsorbate takes places at specific homogeneous sites within the adsorbent and valid for monolayer adsorption onto adsorbents. The expression of the applied Langmuir model is given by the Eq 7 [24]:

$$\frac{C_e}{q_e} = \frac{C_e}{q_m} + \frac{1}{q_m b} \quad (7)$$

where, C_e is the equilibrium dye concentration in the solution (mg/L), b is the Langmuir adsorption constant (L/mg), and q_m is the theoretical maximum adsorption capacity (mg/g). The q_m and b can be calculated from the slope and intercept of a linear plot of $\dfrac{C_e}{q_e}$ versus C_e, respectively.

In the Freundlich model, the adsorption of adsorbate occurs on a heterogeneous surface by multilayer sorption and the adsorption capacity can increase with an increase in adsorbate concentration [25]. Freundlich isotherm is represented by the following equation:

$$Lnq_e = Lnk_f + \frac{1}{n} LnC_e \quad (8)$$

where K_f is the equilibrium adsorption coefficient (L/g), and $1/n$ is the empirical constant. The K_f and n values for nanocomposites can be achieved from the intercept and the slop of plotting of Lnq_e against LnC_e (Figure 8). The all expressions in Langmuir and Freundlich equations and equilibrated dye adsorption of all nanocomposites were calculated according to experimental data and summarized in Table 3. In accordance the high correlation coefficient in Freundlich equation ($R^2 > 0.96$), it depicts that Freundlich isotherm is the best fit of experimental data than the Langmuir model. Considering the results, it is concluded that the adsorption of CV onto nanocomposites take places through heterogeneous surface by multilayer sorption. In Freundlich model, when n values being between 1 and 10, the removing process will be beneficial adsorption [26]. The n values for nanocomposite and clay-free superabsorbent are bigger than 1 and indicate that both samples are favorable for corresponding adsorption. Also, the k_f value for nanocomposites obtained higher than that of clay-free superabsorbent and showed an improvement in adsorption process. In fact, according to k_f values, the adsorption intensity of CV dye on the nanocomposite is higher than the clay-free superabsorbent.
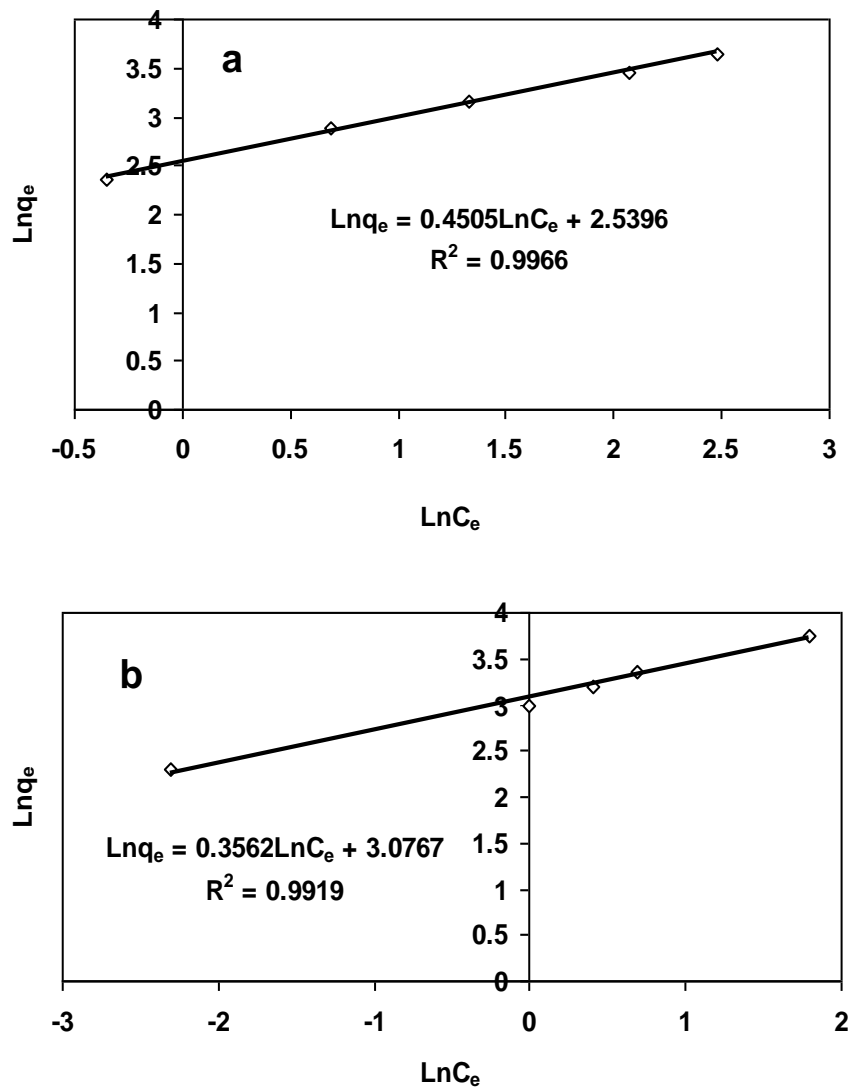
Figure 8 Freundlich isotherms for the adsorption of CV onto (a) clay-free superabsorbent, and (b) Clay8 nanocomposite

Table 3 Isotherm parameters for adsorption of CV onto clay-free superabsorbent and nanocomposite superabsorbent.

Isotherm	Parameters	Samples	
		Clay0	Clay8
Freundlich Model	n, g/L	2.2	2.8
	k_f, mg/g	12.6	21.7
	R^2	0.9966	0.9919
Langmuir Model	q_m, mg/g	55.8	48.3
	b, L/mg	0.23	1.56
	R^2	0.9637	0.9585

Conclusions

Sodium montmorillonite was introduced into carrageenan-based superabsorbent to improve water absorbency and the resultant nanocomposites were applied for removing cationic CV dye from water. The results of the study are as below:

-According to XRD studies, the type of clay dispersion in nanocomposite matrix was achieved as exfoliated form. The SEM micrographs showed that inclusion of Na-MMt can affect the superabsorbent surface.

-Water absorbency capacity of nanocomposites was studied by changing the clay content. An increment in water absorbency was observed up to 8 wt% of Na-MMt due to mobile ions in the nanoclay that can cause an increase in osmotic pressure. At high content of nanoclay, the water absorbency was decreased that can be attributed to the acting of nanoclay as multifunctional crosslinker. Optimum water absorbency was achieved at 8 wt% of Na-MMt nanoclay.

- The obtained nanocomposites were examined to remove of CV dye from water. The results showed that the speed of dye removal was increased by inclusion of Na-MMt into superabsorbent.

- The results showed that the pseudo-second-order adsorption kinetic was predominated for the adsorption of CV onto nanocomposites.

- Freundlich model was obtained as the best model for the adsorption of CV onto nanocomposites.

References

1. Kiani, G.R., Sheikhloie, H., Arsalani, N., *Desalination*, 269 (2011) 266.
2. Eshel, H., Dahan, L., Dotan, A., Dodiuk, H., Kenig, S., *Polym. Bull.*, 61 (2008) 257.
3. Kost, J., Encyclopedia of Controlled Drug Delivery, Mathiowitz E (Ed), Wiley, New York, 1999.
4. Bulut, Y., Akcay, G., Elma, D., Serhatli, I.E., *J. Hazar. Mater.*, 171 (2009) 717.
5. Hamidi, M., Azadi A., Rafiei, P., *Adv. Drug Deliver. Rev.*, 60 (2008) 1638.
6. Jiuhui, Q., *J. Environ. Sci.* 20 (2008) 1.
7. Haraguchi, K., *Curr. Opin. Solid St. M.*,11 (2007) 47.
8. Liu, P., Zhang, L., *Sep. Purif. Technol.*, 58 (2007) 32.
9. Dalaran, M., Emik, S., Guclu, G., Iyim, T.B., Ozgumus, S., *Polym. Bull.*, 63 (2009) 159.
10. Li, P., Siddaramaiah, Kim, N.H., Yoo, G.H., Lee, J.H., *J. Appl. Polym. Sci.*, 111 (2009) 1786.
11. Wang, W., Wang, A., *Carbohyd. Polym.*, 82 (2010) 83.
12. Ekici, S., Isikver, Y., Saraydın, D., *Polym. Bull.*, 57 (2006) 231.
13. Abou-Taleba, M.F., Hegazya D.E. Ismaila, S.A., *Carbohyd. Polym.*, 87 (2012) 2263.
14. Odian, G., Principles of Polymerization, Wiley, New Jersey, 2004.
15. Liu, P.S., Li, L., Zhou, N.L., Zhang, J., Wei S.H., Shen, J., *J. Appl. Polym. Sci.*, 102 (2006) 5725.
16. Junqian, L., Jinhua, W., Ping, L., Xiangde, W., Bo, Y., *Desalin. Water Treat.*, 39 (2012) 70.
17. Li, A., Zhang, J., Wang, A., *J. Appl. Polym. Sci.*, 103 (2007) 37.
18. Darvishi, Z., Kabiri, K., Zohuriaan-Mehr, M.J., Morsali, A., *J. Appl. Polym. Sci.*, 120 (2011) 3453.
19. Al, E., Guclu, G., Iyim, T. B., Emik, S., Ozgumus, S., *J. Appl. Polym. Sci.*, 109 (2008) 16.
20. Buchholz, F.L., Superabsorbent Polymers: Science and Technology, Buchholz, F.L. and Peppas, N.A. (eds). ACS symposium series 573, American Chemical Society: Washington DC, 1994.
21. Omidian, H., Hashemi, S.A., Sammes, P.G., Meldrum, I., *Polymer*, 39 (1998) 6697.
22. Tsai, W.T., Lai, C.W., Hsien, K.J., *J. Colloid Interf. Sci.*, 263 (2003) 29.
23. Zhu, X., Jiang, X., Cheng, S., Wang, K., . Mao, S., Fan L.J., *J. Polym. Res.*, 17 (2010) 769.
24. Rohns, J., Rao, V., *Int. J. Polym. Mater.*, 60 (2011) 766.
25. Ahalya, N., Kanamadi, R.D., Ramachandra, T.V., *Electron J. Biotechn.*, 8 (2005) 258.
26. Kadirvelik K., Namasivayam, C., *Environ. Technol.*, 21 (2000) 1091.